4ICEGE Thessaloniki-GREECE 2007

4th International Conference on
Earthquake Geotechnical Engineering
June 25-28, 2007
Paper No. 1613

NUMERICAL SIMULATIONS OF THE GROUND DEFORMATION RECORDED IN THE HISTORICAL TOWN OF GERACE DURING THE SEISMIC EVENTS IN CALABRIA (1783)

Antonio COSTANZO [1], Anna D'ONOFRIO[2] and Francesco SILVESTRI[3]

ABSTRACT

The case history presented is referred to the historical town of Gerace, located in Calabria (Southern Italy) on a cliff constituted by soft rocks overlying a thick clay shale, characterised by continuous erosion processes affecting ground deformation and slope instability. Some of these phenomena may be attributed to the unusual sequence of five strong earthquakes (M= 5.1 to 6.9) occurred at the beginning of 1783; the present study aims to reproduce by numerical modelling the entire seismic sequence. The reference input motions were obtained by means of a seismic hazard analysis carried out through both a 'macroseismic' and a 'seismogenic' approach. The geotechnical characterisation of the different soils was obtained by combining data taken from field (Down-Hole, MASW, SASW) and laboratory static and dynamic (RC, CTS) tests. The seismic response of the cliff and valley area was simulated by one-dimensional total stress (EERA) and two-dimensional effective stress (FLAC) analyses. The results of both methods permitted to assess the influence of the topography on the site response; also, the effective stress analyses permitted to justify the occurrence of accumulated large deformations following the seismic sequence, reported by the chronicles.

Keywords: Ground deformation, Historical earthquakes, Numerical modelling; Site effects

INTRODUCTION

In Italy several historical towns, settled on top of rock slabs usually overlying a more deformable clayey substratum, are highly exposed to both hydrogeological and seismic risk (e.g. Fenelli et al., 1998; Costanzo et al., 2004; Pagliaroli, 2006).

The case history presented in this study is referred to the historical centre of Gerace, located in the most hazardous seismic zone in Calabria (Southern Italy). The outstanding location of the cliff (Figure 1) favoured the settling of different communities; since the oldest greek colonies to byzantine, arabian, norman and suevian dominations; all of them left evidences of historical heritage, testified by different architecture styles. Italian government and UNESCO decided to impose monumental protection for the historical and artistic value of the centre. Therefore, the site was included as a case study in the framework of the *INGV-S3 Research Project*, promoted by *National Institute of Geophysics and Vulcanology* (INGV) and funded by the *Department of Civil Protection* (DPC) of the Italian Government. In such a context, it seemed appropriate to evaluate the seismic response of the town to the maximum historical earthquake, i.e. referring to the strong seismic sequence of Calabria in 1783.

[1] Ph.D. Student, DDS, University of Calabria, Rende (CS), Italy, Email: acostanzo@dds.unical.it
[2] Professor, DIG, University "Federico II", Napoli, Italy. Email: donofrio@unina.it
[3] Professor, DDS, University of Calabria, Rende (CS), Italy. Email: f.silvestri@unical.it

Figure 1. Landscape view of Gerace cliff and sketch of unstable areas.

SUBSOIL CONDITIONS

Gerace is located at about 480m a.s.l. on a cliff oriented in direction NW-SE, between the basins of two rivers, characterised by continuous gully erosion affecting the slope instability of the valley borders. The upper part of the cliff is formed by a slab constituted, in sequence, by a thick layer of Pliocene calcarenites and sands (about 70m altogether), overlying a deep formation of clayey marls (around 90m), which in turn rests on a relatively thinner (30m) layer of interbedded sands and conglomerates. The slab floats on a deep layer of Oligocene varicoloured clay shales, with an estimated thickness of about 200m. The current geomorphological setting is the result of the intense erosion processes, producing the progressive removal of the soils overlying the clay formation (Monteleone, 1993).

The cliff of Gerace has been for a long time affected by instability problems, evidenced by cracks, local falls, slides and flows. In last years, such movements have been continuously requiring contingent countermeasures, consisting of installation of anchors and buttresses (see Fig.1). Nevertheless, large scale geomorphological studies suggested that all these scattered phenomena can be viewed as shallow evidences of a deep gravitational seating, located in the clay shale formation and extending up to the superjacent soil layers (Monteleone, 1993). The chronicles report that most of the instability phenomena have been triggered by intense rainfalls (Petrucci & Polemio, 2000); however, there are records of repeated large deformations and landslides occurred after strong earthquakes (Romeo & Delfino, 1997).

The geological map in Figure 2a shows the borders of the different formations, as reported by Monteleone (1993), as well as the locations of previous and recent subsoil investigations.

In 1997 several boreholes of variable depths and inclination were executed along the ridge of the cliff (white dots in Fig.2a), for the design of stabilisation works committed by the Municipality; they allowed to take numerous calcarenite samples, tested in laboratory in unconfined compression. In the same period, further investigations, including cross-hole tests, were planned in the middle of the old town centre for the restoration of the Cathedral (grey dots). Two drillings as deep as 120 and 200m (black dots) allowed to identify the complete subsoil layering, down to the varicoloured clays, and detected the groundwater table at the top of the clayey marls. On such a basis, the stratigraphic sections in Figs. 2b,c were sketched.

Recently, more data have been collected from a number of shallower investigations in the lower SE part of the town, for the design of further stabilisation works (red dots in Fig.2a), including down-hole profiles and laboratory tests on the sands and marls. Additional data were available from seismic refraction surveys (green dots) for design investigations for the construction of a theatre in the same area. The authors planned two more investigation sites, one again in this SE area, and another in the SW river valley, where varicolour clays outcrop (blue dots); their purpose was to execute seismic shallow and borehole tests and to retrieve deep undisturbed samples. Shallow samples of calcarenite

and weakly cemented sand were also extracted from excavation pits along fresh slope faces (purple dots).

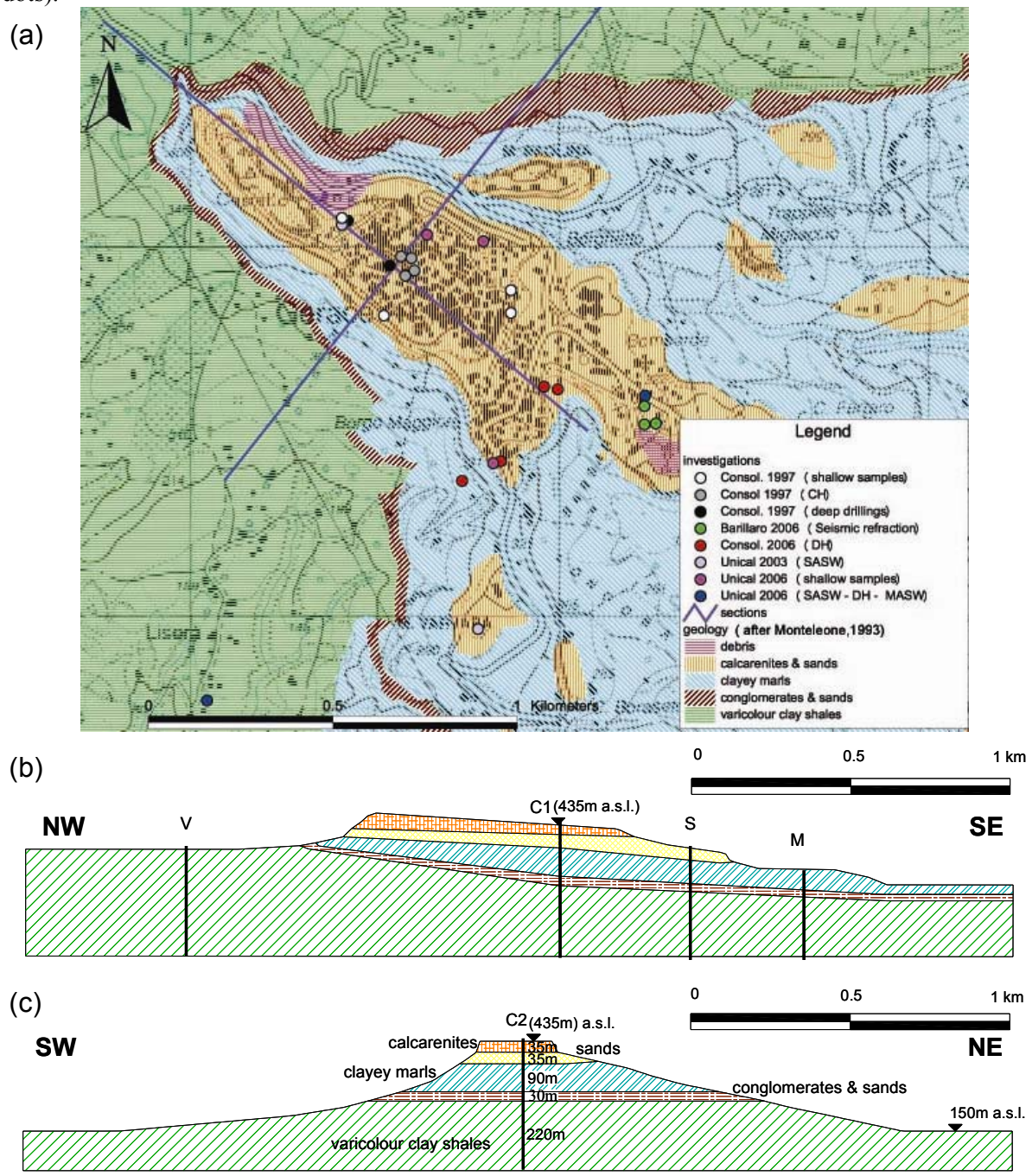

Figure 2. Geological map with investigation sites (a) and sections SW-NE and NW-SE (b).

THE REFERENCE SEISMIC SCENARIO

The historical Calabrian seismic sequence in 1783

In less than sixty days of 1783, since February, 5 to March, 28, Southern Calabria was struck by five strong earthquakes, with magnitudes between 5.9 and 6.9 (Figure 3). The sequence caused the destruction of many towns (Carbone-Grio, 1887) as well as the environmental upset (Cotecchia et al., 1986). The damage suffered at Gerace was characterised by an anomalous evolution: in fact, while the seismic epicentres shifted northwards, the site showed repeated damages and ground deformations (cf. Fig.3), mainly defined as 'landslides' in the Italian Strong Motion Catalogue (Boschi et al., 2000).

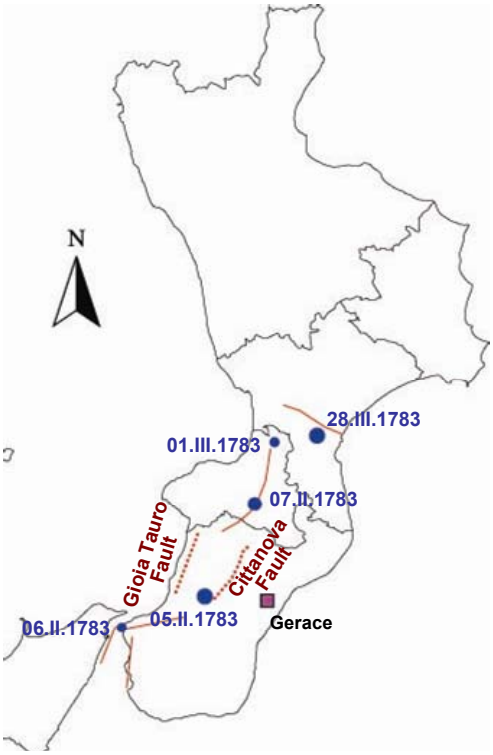

Event	M_s	epic. distance (km)	I_S (MCS)	n_d	a_{max} (g)
05.II.1783	6.91	22.04	8.0	2	0.204
06.II.1783	5.94	51.76	-	-	0.039
07.II.1783	6.59	34.42	7.5	2	0.101
01.III.1783	5.92	55.95	-	-	0.036
28.III.1783	6.94	60.68	7.0	2	0.087

Figure 3. Epicenters and magnitudes of the Calabrian seismic sequence in 1783; site intensity (I_S), number of damages (n_d) and values of a_{max} computed through hazard analyses.

The area of Southern Calabria is characterised by complex and apparently uncertain seismogenic sources. As a matter of fact, the distribution of macroseismic intensity and environmental damages induced to ascribe the generation of each event of the whole sequence to different faults (shown in Fig.3), showing an apparent interaction among them. Different assumptions were formulated in literature on the source location for the first earthquake on 5-II-1783, attributed either to 'Cittanova Fault' (Galli & Bosi, 2002) or to 'Gioia Tauro Fault' (Peruzza et al., 1997). Such uncertainty induced the authors to compare the two hypotheses, assuming both a 'macroseismic' and a 'seismogenic' approach (Costanzo, 2006) to estimate the reference ground motion parameters required for the site seismic response (SSR) analyses.

With the 'macroseismic approach', using the epicentral distance and magnitude from Italian Parametric Strong Motion Catalogue (Gasperini et al., 2004) and the attenuation law by Sabetta & Pugliese (1987), the peak horizontal acceleration (a_{max}) estimated at Gerace resulted 0.204*g*.

Following a 'seismogenic approach', the earthquake magnitude was alternatively estimated on the basis of the surface rupture length (Wells & Coppersmith, 1994), and the distance of Joyner & Boore (1981) computed from the fault geometry; hence, a_{max} was evaluated by the attenuation law of Ambraseys (1995), assuming a focal depth equal to 10 km, as indicated by Seismogenic Italian Zonation (Meletti et al., 2004). Under such hypotheses, a_{max} resulted between 0.183 and 0.197*g* for Cittanova fault, and 0.195 to 0.205*g* for Gioia Tauro fault.

Summarising, the two approaches yielded very close evaluations of the motion amplitude; the macroseismic approach was then extended to evaluate a_{max} for all the other events (Figure 3), for which information about geometry of faults was absent or incomplete. Finally, the generalised attenuation relationship by Pugliese & Sabetta (1989) allowed to estimate reference response spectra for the seismic events, to help in the choice of compatible accelerograms.

Selection of natural accelerograms as input

On the basis of the above parameters, fixing suitably restricted ranges of magnitude and distance, compatible seismic records were selected as possible input motions from seismic databases. Table 1 reports 9 different seismic records sorted out for the simulation of the first event (M_S=6.91).

Table 1. Records selected from seismic databases

Earthquake	Date	M_S (M_W)	Station	component	D_{rms}	F_{sc}
Landers, USA	28.VI.1992	7.5	Morongo Valley - Fire Stn 461	135	0.090	1.505
Northridge, USA	17.I.1994	7.1	Wonderland, California	185	0.104	1.092
Loma Prieta, USA	18.X.1989	7.1	Sierra Pt., San Francisco	205	0.108	1.998
Imperial Valley, USA	15.X.1979	6.9	Delta	262	0.125	0.863
El Salvador	13.II.2001	*6.6*	Col. Ext. S. Jose, San Salvador	0 (N-S)	0.143	1.491
Montenegro	01.IV.1979	7.0	Petrovac - Hotel Oliva	N-S	0.144	0.812
Duzce, Turkey	12.XI.1999	*7.1*	Duzce	90 (E-W)	0.145	0.738
Irpinia, Italy	23.XI.1980	6.9	Sturno	N-S	0.148	0.883
Chi Chi, Taiwan	20.IX.1999	7.6	TCU046	E-W	0.148	1.574

To select the most reliable accelerograms, the approach suggested by Bommer & Acevedo (2004) was followed, computing the amplitude scale factor, F_{sc}, between the reference and the selected motion:

$$F_{sc} = \frac{a_{0,\max}}{a_{S,\max}} \tag{1}$$

and the root mean square parameter, D_{rms}:

$$D_{rms} = \frac{1}{N}\sqrt{\sum_{i=1}^{N}\left(\frac{a_0(T_i)}{a_{0,\max}} - \frac{a_S(T_i)}{a_{S,\max}}\right)^2} \tag{2}$$

In eqn. (2), $a_0(T_i)/a_{0,\max}$ and $a_S(T_i)/a_{S,\max}$ are the normalized spectral ordinates at a period T_i of the reference and selected motion, N is the number of periods used. The parameter D_{rms} supplies a quantitative evaluation of the similarity between the frequency contents. The first four records in Table 1, characterised by the lowest values of D_{rms} were preferred to the others, although the scale factors resulted in two cases (Landers, Loma Prieta) not very close to unity. Figure 4 shows the spectral compatibility among the reference input motion and the selected accelerograms.

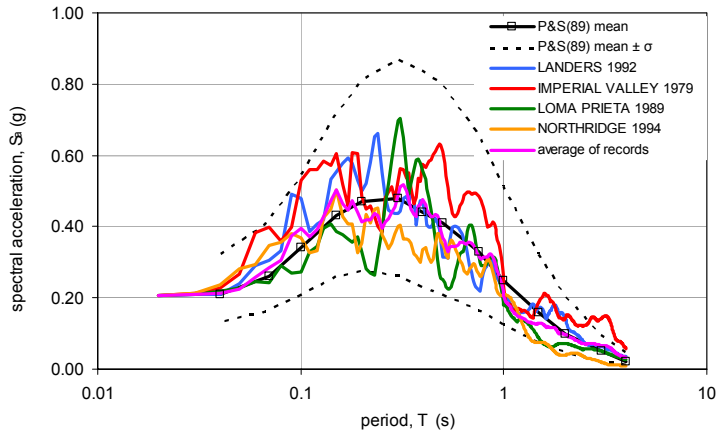

Figure 4. Spectral compatibility among selected accelerograms

GEOTECHNICAL CHARACTERISATION

The subsoil model for the dynamic seismic response analyses was obtained by combining the data collected from the previous investigations and experimental results gathered by the authors through dynamic in situ (Down-Hole, MASW and SASW) and laboratory tests. All the laboratory tests were carried out at University of Naples by means of a Resonant Column/Torsional Shear device (THOR, d'Onofrio et al., 1999) which allowed to characterise both linear and non-linear cyclic behaviour of the different soil units.

Shear wave velocity measurements on the clayey marl (Figure 5a) were obtained by couples of Down-Hole tests located uphill (U) and downhill (D) along two different slopes (sites A and B), where the cliff has recently shown instability. The profiles reported in Fig.5a show values V_S increasing with depth down to about 10m, where the subsoil is constituted either by loose covers of sands (uphill), or by weathered marl (downhill). For the U-A profile, the DH measurements are comparable to those from Resonant Column (RC) tests on an undisturbed sample taken at about 2.5m depth. A multi-stage consolidation test in a stress range 200-900 kPa on the laboratory sample permitted to define the law of variation of V_S with depth, reported in Fig.5a with a dashed line. As a first approximation, a constant value of 750 m/s was assumed for this soil in the geotechnical model for the SSR analyses (Figure 5d).

Surface (SASW, MASW) and borehole (Down-Hole) seismic in situ tests were carried out by the authors in two sites, where the sand and varicoloured clay shale units outcrop (cfr. Fig. 2a).The shear wave velocity profiles in the sand subsoil showed an overall good agreement among the different testing techniques (compared in Figure 5b) and with the values found for the covers of the marl formation (verticals UA and UB in Fig. 5a). The average value of V_S = 400 m/s was then attributed to the sand formation in the geotechnical model (Figure 5d). The DH test allowed to identify the presence of a stiffer layer of calcarenite at 8-10m depth, confirmed by the stratigraphic log, but not detected by the surface waves profiles. On the basis of such measurement, a value of 750 m/s was assigned to the uppermost calcarenite formation (Figure 5d).

The major experimental efforts were spent in the characterisation of the varicolour clay shale, at the test site in the SW valley at the toe of the cliff. A first borehole was conditioned for the installation of two Casagrande piezometers, which detected the groundwater table at 10 m depth. Another borehole was faced for the execution of DH tests. Just like for sand, the different geophysical tests also provided comparable V_S profiles (Figure 5c). Four undisturbed samples were retrieved from the same borehole, in order to carry out Resonant Column and Cyclic Torsional Shear (CTS) tests. The experimental programme was addressed to characterise the dependency of the cyclic stress-strain behaviour on the variable in situ stress state and history sustained by the varicoloured clay: namely, the overburden compression for the formation underlying the cliff, and the swelling, due to the erosion, for that outcropping in the valleys. To reproduce in the RC-TS tests the in-situ stress paths undergone by the highly compressed clay shale, two specimens were subjected to a multi-stage consolidation sequence, starting from the estimated in situ stress state (≈400 kPa) and then loading to 800 and 1200 kPa. Another specimen, instead, was left swelling under a mean effective stress of 200 kPa, lower than the estimated overburden pressure.

In order to differentiate the V_S profiles under the cliff and in the surrounding valley, the dependency of the small strain stiffness, G_0, on stress state and history was modelled following the approach introduced by Rampello et al. (1994). The relationship between G_0, the current stress state and the stress history of the soil can be expressed as follows:

$$\frac{G_0}{p_r} = S \cdot \left(\frac{p'}{p_r} \right)^n \cdot \left(\frac{p'_y}{p'} \right)^m \tag{3}$$

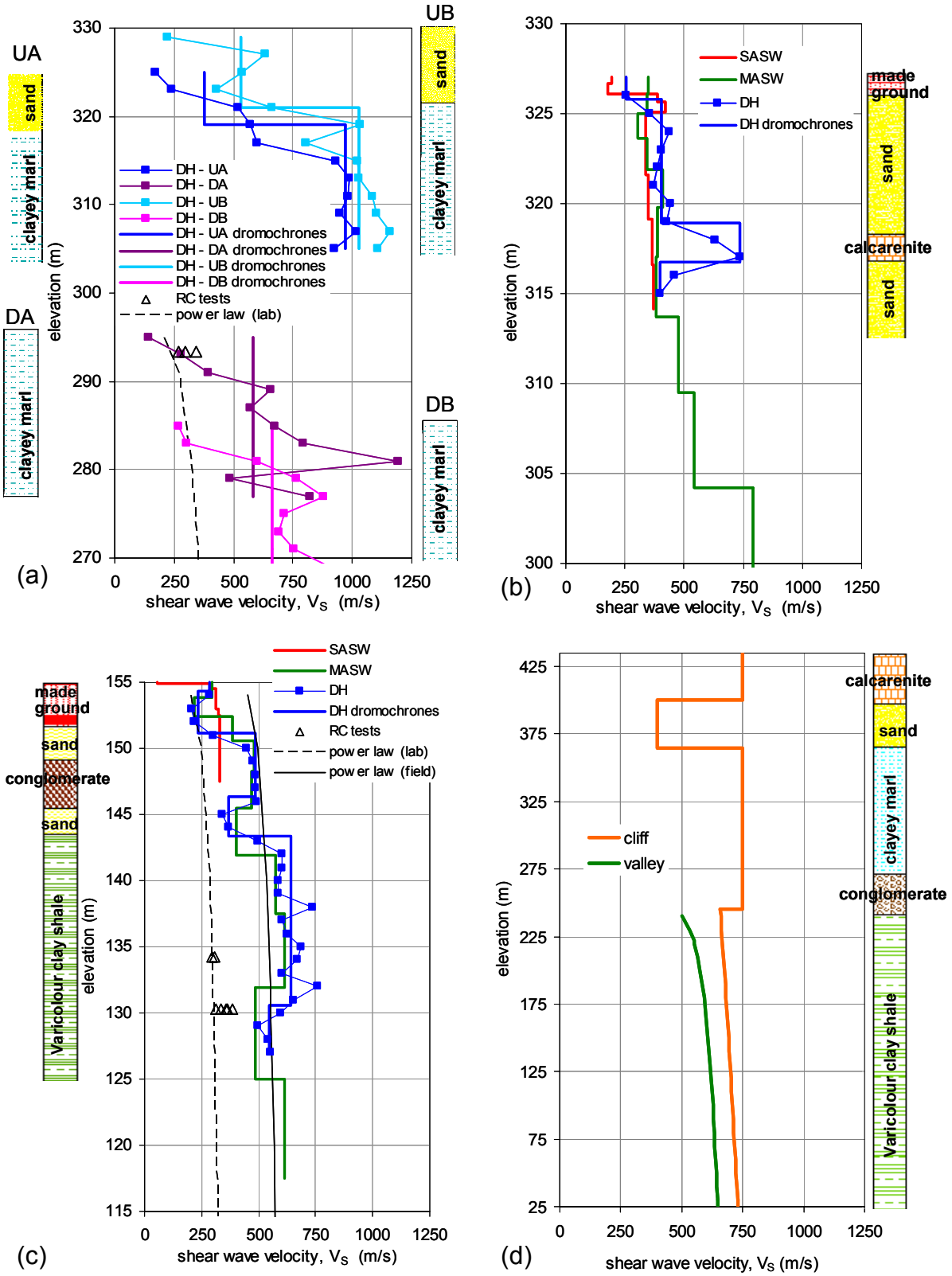

Figure 5. Shear wave velocity profiles measured at outcrops of marl (a), sand (b) and varicolour clay (c); subsoil model assumed for the SSR analyses (d).

In eqn. (3), the coefficient S represents the stiffness of the clay when normally consolidated at a reference stress state $p'=p_r$ (typically taken equal to 1 kPa or to the atmospheric pressure), the exponent n depends on the rate of variation of G_0 with the normal consolidation stress, and m accounts

for the dependency of G_0 on the overconsolidation ratio. With reference to a given unloading-reloading compression path, characterised by a given gross yield stress p'_y, eqn. (3) can be re-arranged as follows:

$$G_0 = S \cdot (p_r)^{1-n} \cdot (p'_y)^m \cdot (p')^{n-m} \tag{4}$$

The RC measurements of the small strain shear modulus, relevant for the overconsolidated states due to erosion in the valley, were fitted adopting a power function:

$$G_0 = A \cdot (p')^b \tag{5}$$

By expressing G_0 in MPa and p' in kPa, A was found equal to 49 and b=0.25. By comparing the power functions (4) and (5), it can be observed that the exponent b is equal to $(n-m)$, while the coefficient A corresponds to $S(p_r)^{1-n}(p'_y)^m$, and, therefore, it is proportional to the gross yield stress. The normally consolidated behaviour of the clay shale under the cliff was modelled by the equation:

$$G_0 = S \cdot (p_r)^{1-n} \cdot (p')^n = A' \cdot (p')^n = \frac{A}{(p'_y)^m} \cdot (p')^n \tag{6}$$

Due to the lack of experimental data relevant to normally consolidated states, some assumptions had to be made. The gross yield stress p'_y was assumed to be equal to the overburden stress acting on the clay shale lying under the cliff, estimated to be about 2.88 MPa; the exponent m was taken equal to 0.35 from literature data, averaging values relevant to natural clays of Southern Italy with comparable plasticity and macro-structure (d'Onofrio et al., 1998). Thereafter, the power law (6) could be defined by assuming $A'=A/(p'_y)^m \approx 3$ and $n=b+m=0.6$.

By expressing eqns. (5) and (6) in terms of $V_S(z)$ relationships, the laboratory values were then scaled to those measured in the field, to account for sampling disturbance and reconsolidation procedure. Finally, the shear wave velocity profiles drawn in Figure 5c-d could be obtained, highlighting the lower velocity values in the valley (450-650 m/s) due to the swelling of the varicolour clay, compared to those underneath the slab (660-725 m/s).

The laboratory tests results also allowed to describe the non-linear behaviour of the fine-grained soils. Figure 6a-b reports the variations with shear strain, γ, of the normalised shear modulus, G/G_0, and the damping ratio, D, of clayey marls and varicolour clays, respectively. The data points, taken from CTS tests results, were fitted by the hyperbolic model (Hardin & Drnevich, 1972), to be used in the numerical SSR analyses described in the following section. The data relevant to the clay shales under swelling and compression loading paths were expressed through different relationships, to account for the higher degree of non-linearity and damping values pertaining to the valley formations. The same graphs also show the curves for the sands (Fig. 6a) and conglomerates (Fig. 6b), as taken from literature indications relevant to soils with comparable lithology, respectively given by Seed & Idriss (1970) and Marcellini et al. (1995).

Table 2 shows a summary of the parameters used for the numerical simulations discussed later. The shear wave velocity V_S is set constant for all formations, except for the varicolour clay shales, where it varies with depth. The measurements of the compression wave velocity V_P in the down-hole tests allowed to set the values of Poisson's coefficient ν for all soils. The shear and compression moduli, G and K', were obtained on the basis of V_S and V_P, and of the average unit weight γ measured on undisturbed samples. The small strain damping D_0 was assumed on the basis of CTS tests for the fine-grained soils, from literature in the other cases.

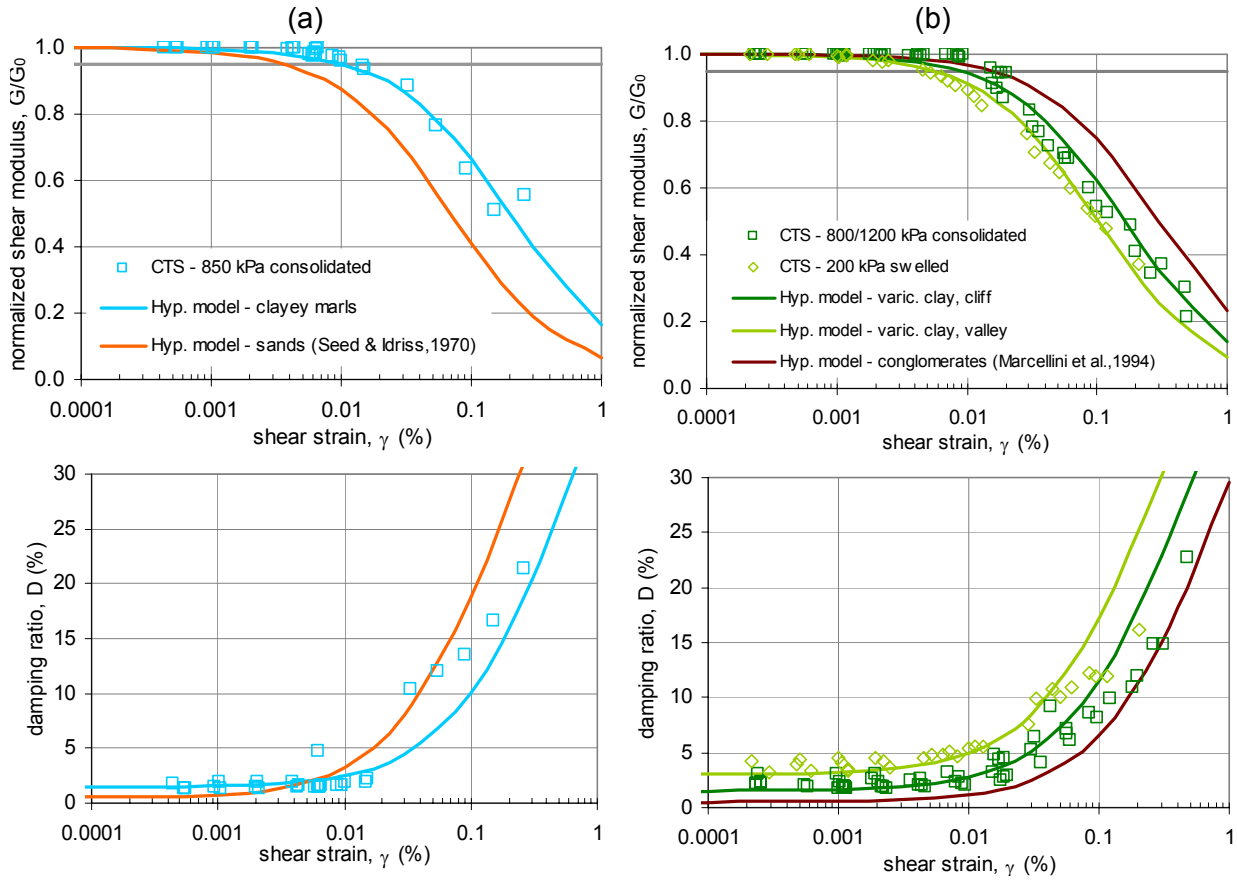

Figure 6. Strain-dependent equivalent parameters resulting from literature and experimental data for sand and marl (a), conglomerate and varicoloured clay (b).

Table 2. Soil parameters for SSR analyses.

material	G (MPa)	K' (MPa)	ν	γ (kN/m^3)	V_S (m/s)	D_0 (%)	φ' (°)	c' (kPa)	γ_r (%)	γ_v (%)
calcarenite	956.3	2071.9	0.300	16.69	750	0.5	45	700	linear	
sand	272.0	589.3	0.322	16.94	400	0.5	30	0	0.07	0.04
clayey marl	1012.5	2193.8	0.332	18.05	750	2	30	37	0.2	0.1
conglomerate & sand	1125.0	2437.5	0.285	19.51	750	0.5	35	50	0.3	0.16
varicolour clay (cliff)	914.8	4268.9	0.400	21.00	660	1.5	25	0	0.164	0.068
	1100.8	5136.9			725					
varicolour clay (valley)	425.3	1984.5	0.361	20.87	450	3	25	0	0.103	0.052
	887.3	4140.5			650					
bedrock	4950.0	10725.0	0.300	22.00	1500	linear				

The calcarenite was assumed as a linear material, as well as the bedrock, which was assumed to be a stiff rock half-space, set at a depth of about 200m on the basis of the previous geological studies. For the non-linear material models, the hyperbolic law is expressed by the reference strain (γ_r), i.e. the value for which G=0.5G_0; the shear-volumetric coupling, instead, is expected to be triggered beyond a volumetric threshold strain, (γ_v), corresponding to the value for which G=0.65G_0. The effective strength parameters, c′ and φ′, for the sand and fine-grained soils were obtained from direct shear tests on undisturbed samples, those for the calcarenites from uniaxial compression tests (cf. Costanzo, 2006); the strength for the conglomerates was assumed on the basis of experience on similar soft rocks (Marcellini et al., 1995).

NUMERICAL SIMULATION OF THE SEISMIC SEQUENCE

Modelling

The seismic response of the cliff and the surrounding valley was simulated by one-dimensional and two-dimensional analyses with different numerical methods. The results of preliminary 1D analyses (Costanzo, 2006) allowed to assess the compatibility of the different codes, namely:

- EERA (Bardet et al., 2000), i.e. 1D total stress linear equivalent analyses in the frequency domain;
- D-MOD_2 (Matasovic, 1995), i.e. 1D effective stress non-linear analyses in the time domain;
- QUAD4M (Hudson et al., 1994), i.e. 2D total stress linear equivalent analyses in the time domain, by the finite elements method;
- FLAC 5.0 (Itasca, 2005), i.e. 2D effective stress linear equivalent analyses in the time domain, by the finite differences method (FDM).

The consistency of the previous methods was verified by comparing the predictions of the dynamic response of a simplified model corresponding to a layered soil column across the cliff. First, the comparison between 1D and 2D modelling showed the effects on the ground response of the impedance contrast between the slab and the underlying clay formation, combined with those of the topography.

Thereafter, to reliably predict the subsoil response to the entire seismic sequence, 2D effective stress analyses by FLAC 5.0 were addressed to reproduce the permanent strains and the eventual generation and partial dissipation of pore water pressure in the different formations. In such analyses, the pre-failure soil behaviour was assumed as linear equivalent visco-elastic, characterised by the small strain parameters and the hyperbolic laws reported in Table 2 and Fig.6; the damping was included in the FDM algorithm according to the well-known Rayleigh formulation, i.e. assuming that the damping tensor [C] is a linear combination of the mass [M] and the stiffness [K] tensors:

$$[C] = \alpha[M] + \beta[K] \tag{7}$$

Coefficients α and β have been chosen according to a double frequency approach (Lanzo et al., 2004), giving the same damping-frequency function as the single frequency method used by the program, and referring to the values of the small strain damping ratio, D_0, reported in Table 2. In these effective stress analyses, soil behaviour at failure was represented by a Mohr-Coulomb plastic envelope, with an non-associated flow rule and hysteresis controlled by the hyperbolic model.

Figure 7 shows the two mesh grids used to model the geological sections in Figure 2; the thickness of the mesh elements was set equal to 7m throughout the whole grid. According to the well-known rule of the thumb by Lysmer & Kuhlemeyer (1969), this size corresponds to a maximum frequency reproduced of about 10Hz, for a soil with V_S=400 m/s, i.e. the lowest value in the subsoil profile (cf. Fig. 5 and Table 2). The seismic input motions, sampled at 0.01 s, were preliminarily low-pass filtered to a frequency of 15 Hz, and the time step in the integration was set equal to $5 \cdot 10^{-5}$ s.

To avoid undesired wave reflections in correspondence to the model boundaries, a ‘quiet boundary’ condition was adopted for the bedrock (Lysmer & Kuhlemeyer, 1969), consisting of viscous dampers acting along normal and tangential directions, whereas ‘free-field boundary’ conditions were used for the lateral contours. These latter consist of one-dimensional columns simulating the behaviour of a lateral semi-infinite medium, linked to the mesh grid through viscous dashpots.

Results

The plots in Fig. 7a-b report the horizontal peak acceleration profiles as obtained from the numerical 2D simulations of the first event, along the two orthogonal sections of the cliff, using the Landers accelerogram, i.e. that showing the best spectral compatibility (see Table 1 and Fig. 3). The time history, scaled to a peak acceleration of 0.20g, was 1D de-convoluted by EERA, resulting in a peak value of 0.15g at bedrock.

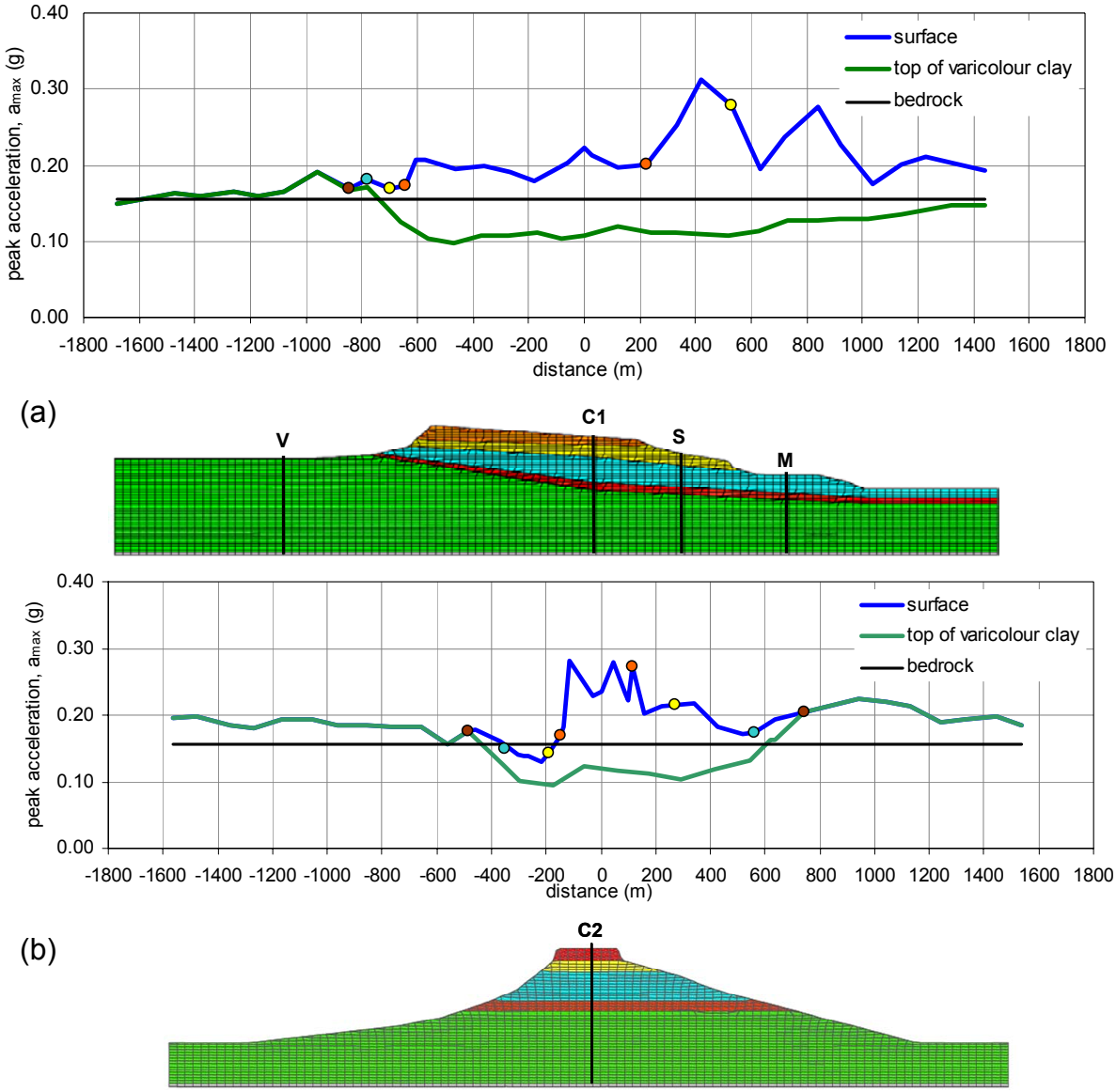

Figure 7. Horizontal peak acceleration profiles along NW-SE (a) and SW-NE (b) sections.

The green lines refer to the accelerations at the top of the varicolour clay, while the blue ones pertain to the values computed at surface; the coloured dots indicate the stratigraphic contacts between different soils. The amplitudes at the top of the clay are significantly lower than the reference input motion (black horizontal lines) for the clay formation underlying the slab, while an apparent amplification is shown along the outcropping clay at the toe of the cliff, more pronounced for the SW-NE section (Fig. 7b). In this latter, the wave focalisation into the narrow hill section clearly induces a significant topographic effect, resulting in a stronger amplification at the top of the cliff; along the SE-NW section (Fig. 7b), characterised by a smoother topographic profile, the interaction between incident and diffracted waves could be responsible for the sequence of amplifications and de-amplifications along the slopes.

The results of the same simulations of the main shock are plotted in Figure 8 as vertical profiles of peak acceleration, shear stress and strain at different reference sites, located along the NW-SE section, at the outcrop of calcarenites (C1), sands (S), marls (M) and varicolour clays (V). The data obtained at the vertical C2, where the two sections intersect, are also shown for comparison.

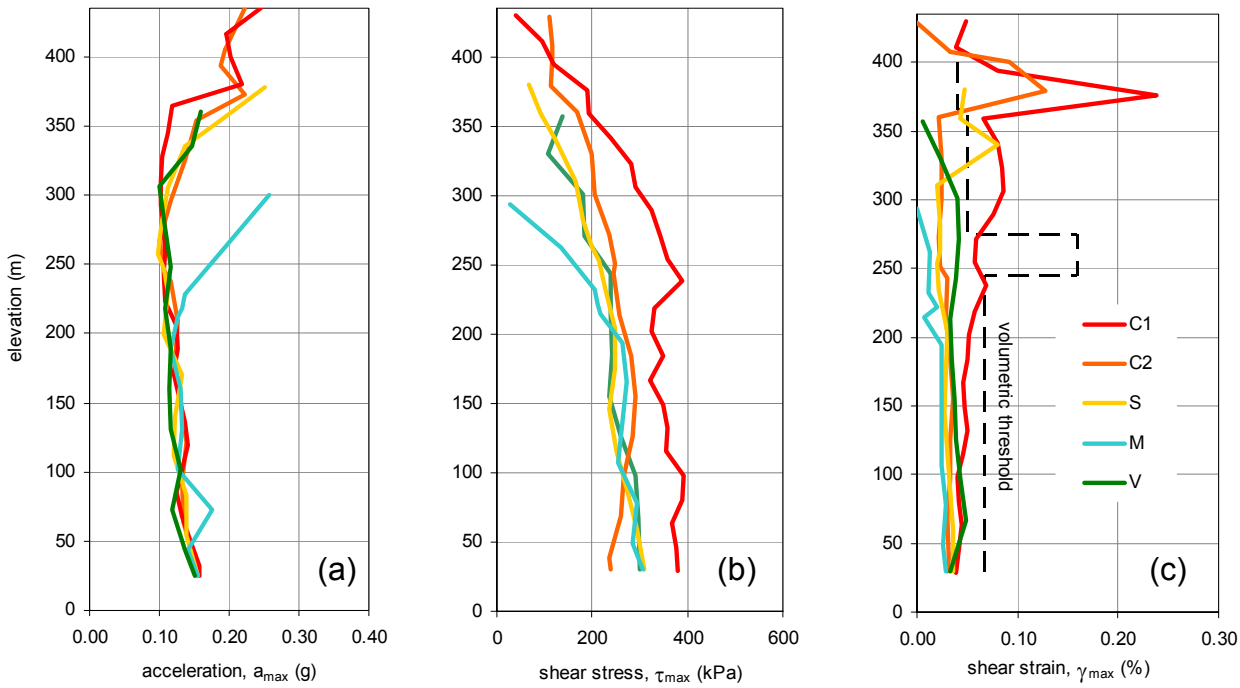

Figure 8. Vertical profiles of peak acceleration (a), shear stress (b) and strain (c) at reference sites.

The profiles of maximum acceleration (a) along the varicolour clay formation show quite similar trends for all the verticals considered, gradually decreasing with elevation; most of the amplification is concentrated along the uppermost 100m, i.e. in the marl and, mostly, in the sand formations. In both axis verticals, C1 and C2, the calcarenites do not significantly modify the peak motion amplitudes. The peak shear stress shown in Fig. 8b were verified to result lower than the strength values; the strain profiles reported in Fig. 8c show that the central verticals C1 and C2 suffer the maximum shear deformations, with values of γ_{max} systematically exceeding γ_v (dashed black line) in the sand and marl layers, along the NW-SE section.

The response spectra in Figure 9a,b show the coupled effects of the stratigraphic and topographic amplifications on the seismic response at surface. In Fig. 9a, the spectral accelerations evaluated at the reference sites in Fig. 7a are compared with the input motion; the varicolour clay shows a quite uniform amplification throughout the entire frequency range, while both marls and sands mostly amplify frequencies between 1-2 Hz, and the calcarenite layer seems to enhance the response at higher periods. The peak spectral acceleration are shown to reach up to 1g at M and S verticals.

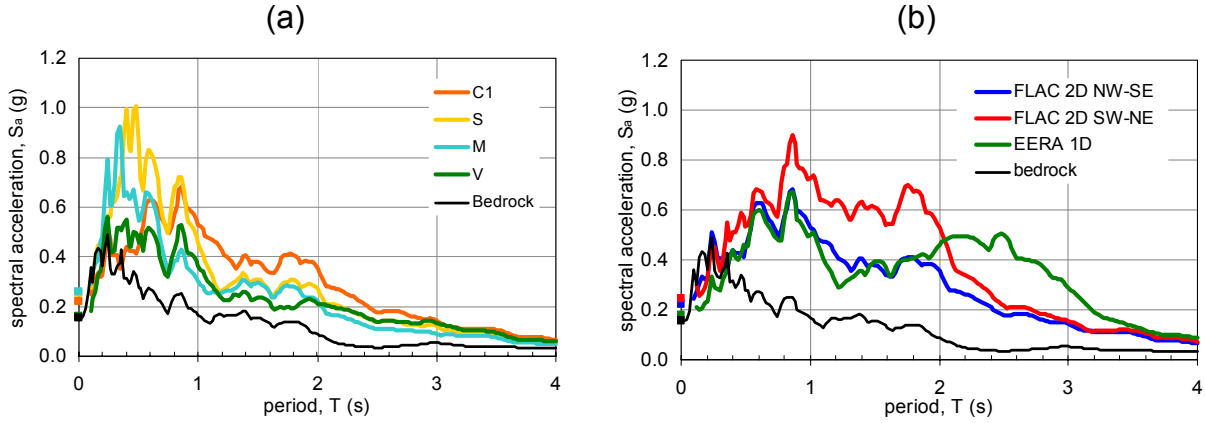

Figure 9. Response spectra showing stratigraphic (a) and topographic (b) amplification.

Figure 9b reports the response spectra predicted at the town center (verticals C1 and C2) by 2D numerical analyses, compared to that obtained by 1D analysis with EERA and to the bedrock motion. Along the NW-SE direction, where the topographic effects are expected to be less significant, the 1D and 2D results are indeed very similar up to about 2 s. However, the 1D analysis shows a strong amplification at about 2.5s, which corresponds to the fundamental frequency of the profile; this anomaly is probably due to an underestimate of resonance damping, inherent in the frequency domain analyses. The higher spectral amplitudes relevant to the NE-SW direction confirm that topographic amplification affects more significantly the transversal section of the hill.

The plastic deformation pattern of the hill, resulting after the entire seismic sequence simulated, resulted practically coincident with that corresponding to the main shock. Contours of residual shear strains along the NW-SE section are shown in Fig.10, overlapped to the picture of Fig.1; the boundary of the calcarenite formation is also drawn. Plastic strains develop throughout the whole sand layer, indicating a tendency to slippage of the calcarenite layer along the contact with the underlying sand. The highest irrecoverable strains concentrate at the NW toe of the hill, and across the soft rock slab, indicating a likely asynchronous motion of three independent calcarenite blocks. It is worth noting that the strains concentrate along the vertical discontinuities which can be nowadays observed in the slab.

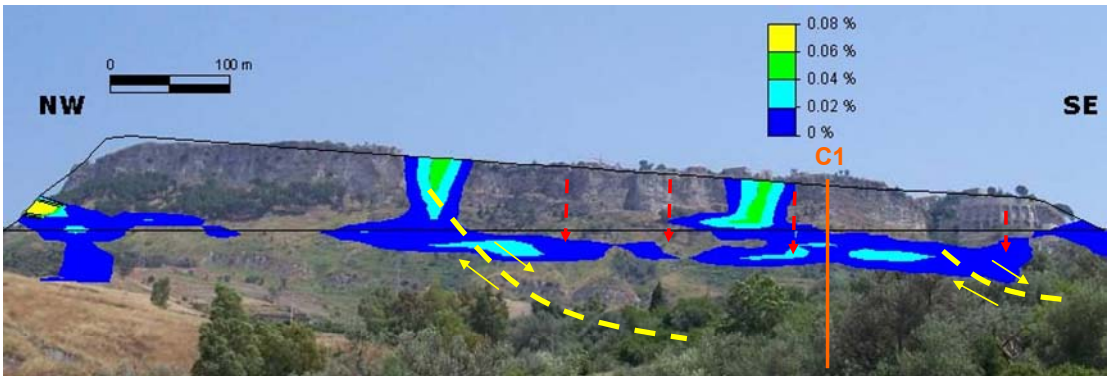

Figure 10. Residual deviatoric strain field after the sequence of earthquakes.

The final deformation pattern of the transversal section of the hill is shown in Figure 11, through displacement contours and vectors. Both graphs show displacements as high as about 1m in the varicolour clay, close to the contact with the conglomerates; the overall distribution seems to highlight the triggering of a rotational slope instability at the base of the hill, due to the increment of inertia forces in the shallowest layers induced by swelling. A rigid sliding of the calcarenite above the sand layer is also detectable at the hilltop.

CONCLUSIONS

A detailed seismic hazard analysis allowed to figure out the main parameters of the historical seismic sequence occurred in Southern Calabria in 1783. Such procedure, used for the simulation of the seismic response of Gerace hill, can be of interest for further seismic risk analysis of other strategic sites in the same area, such as big earth dams (at Castagnara and Siderno sites), and transportation infra-structures such as highways and ports (e.g. Reggio Calabria and Gioia Tauro).

A comprehensive geotechnical characterisation was based on previous investigations available and specifically arranged field and laboratory tests on the different soils and soft rocks characterising the hill. Most of the materials have rather complex behaviour, hence further experimental studies need to be planned in the future. A more complete geological picture is necessary for a better geometrical description of the subsoil model in both longitudinal and transversal directions of the hill. The residual unknowns on the bedrock nature, depth and geometry should be better investigated by for instance deep geophysical surveys. Very recently, an indirect verification of the thickness (about 200m)

assumed for the varicolour clay was obtained by the accelerometric record, taken in the Gerace cathedral, of a deep strong motion event (M_L=5.7, focal depth about 200 km) occurred about 80 km north-west.

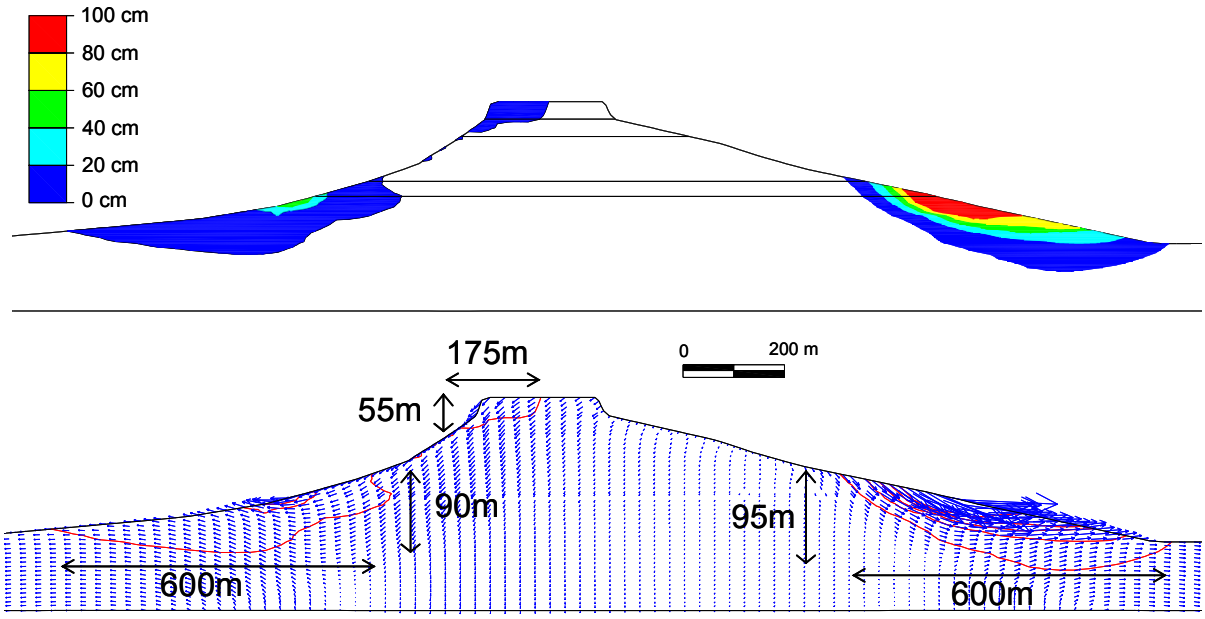

Figure 11. Distribution of permanent displacements after the sequence of earthquakes.

The results of 1D and 2D numerical simulations evidenced the distinct effects of both stratigraphy and topography on the ground motion in the town centre and along the slopes. The computed permanent strains and displacements could justify the occurrence of accumulated large deformations following the seismic sequence, reported by the chronicles. However, a better understanding of geomorphology and groundwater conditions, still not very clear at present, might address more reliable predictions of both hydrogeological and seismic risk of such a precious heritage.

ACKNOWLEDGMENTS

The work is part of the *INGV-S3 Research Project*, promoted by *National Institute of Geophysics and Vulcanology* (INGV) and funded by the *Department of Civil Protection* (DPC) of the Italian Government. The authors are indebted to the DPC and the project team coordinators, Dr. Francesca Pacor and Prof. M. Mucciarelli, for their valuable scientific and administrative support. Profs. J.P. Stewart, G. Lanzo and I. Guerra, Dr. F. Galadini and Dr. P.Tommasi are also warmly acknowledged for the fruitful discussions and suggestions.

REFERENCES

Ambraseys, N.N. “The prediction of earthquake peak ground acceleration in Europe. Earthquake Engineering and Structural Dynamics,” 24(4), 467–490, 1995

Bardet J. P., Ichii K. and Lin C.H. “A computer Program for Equivalent-linear Earthquake Site Response Analyses of Layered Soil Deposits (EERA),” University of Southern California, Department of Civil Engineering, 2000

Bommer J. J. and Acevedo A. B. “The use of real earthquake accelerograms as input to dynamic analysis,” Journal of Earthquake Engineering, 8, special issue 1: 43-91, 2004

Boschi E., Guidoboni E., Ferrari G., Mariotti D., Valensise G. and Gasperini P. “Catalogo dei Forti Terremoti in Italia dal 461 a.C. al 1997 d.C.,” Istituto Nazionale di Geofisica, Storia Geofisica Ambiente, 2000 (in Italian)

Carbone Grio D. “Terremoti di Calabria e Sicilia nel secolo XVIII,” Barbaro editore, Oppido Mamertina (RC), 1884 (in Italian)

Costanzo A. “Risposta sismica e comportamento post-sismico di centri storici su alture rocciose: il caso di Gerace,” D.Sc. Thesis, Università della Calabria, 2003 (in Italian)

Costanzo A., Silvestri F., Lampitiello S., Olivares L., Lanzo G. and Tommasi P. “Vulnerabilità sismica di centri storici su rilievi: i casi di Bisaccia, Orvieto, Gerace,” XI Congresso Nazionale “L’Ingegneria Sismica in Italia” Genova, ANIDIS, Roma, 2004 (in Italian)

Costanzo A. “ Analisi di fenomeni deformativi di pendii e rilievi in condizioni sismiche : il caso di Gerace,” Ph.D.teshis, Università della Calabria, 2006 (in Italian)

Cotecchia V., Guerricchio A. and Melidoro G. “The Geomorphogenetic Crisis Triggered by the 1783 Earthquake in Calabria (Southern Italy),” Symposium: Engineering Geology Problems in Seismic Areas,Volume 6, Bari, 1986

D’Onofrio A., Olivares L. and Santucci de Magistris F. “Influence of soil structure on the behaviour of two stiff italian clay in the pre-failure range,” 2nd International Symp. on “The geotechnics of Hard Soils and Soft Rocks” Balkema, Rotterdam 1:497-506, 1998

D'Onofrio A., Sivestri F. and Vinale F. “New torsional shear device,” ASTM. Geotechnical Testing Journal, vol 22(2), 107-117, 1999

Fenelli, G.B., Pellegrino, A. and Picarelli, L. “Stability problems of old towns built o relict plateaux on clay deposits”, Proc. Int. Symp. on Geotechnical Engineering for the Preservation of Monuments and Historic Sites, Napoli. 163-173. Rotterdam: Balkema, 1998

Galli P. and Bosi V. “Paleoseismology along the Cittanova fault: Implications for seismotectonics and earthquake recurrence in Calabria (Southern Italy),” Journal of Geophysical Research, Vol. 107, No. B3, 2044, ETG 1 pp.1-19, 2002

Gasperini P., Camassi R., Mirto C. and Stucchi M. “Catalogo Parametrico dei Terremoti Italiani. Versione 2004 (CPTI04),” Gruppo di lavoro Istituto Nazionale di Geofisica e Vulcanologia (INGV), Roma, 2004 (in Italian)

Hardin B.O. and Drnevich V.P. “Shear modulus and damping in soils: design equations and curves,” Proc. Journal of the Soil Mechanics and Foundations Division, ASCE. 98(SM7):667-692, 1972

Hudson M., Idriss I.M. and Beikae M.. “QUAD4M: a computer program to evaluate the seismic response of soil structures using finite element procedures and incorporating a compliant base,” Center for Geotechnical Modeling, Department of Civil and Environmental Engineering, University of California Davis, Davis California, 1994

Itasca Consulting Group,”Flac 5.0 USER’S Manual,” Minneapolis, Minnesota, 2005

Joyner, W.B.and Boore D.M. “Peak horizontal acceleration and velocity from strong-motion records including the records from the 1979 Imperial Valley, California, earthquake,” Bull. Seism. Soc. Amer., 71, 2011-2038, 1981

Lanzo G., Pagliaroli A. and D’Elia B. “Influenza della modellazione di Rayleigh dello smorzamento viscoso nelle analisi di risposta sismica locale,” XI Congresso Nazionale “L’ingegneria Sismica in Italia”, Genova. ANIDIS, Roma, 2004 (in Italian)

Lysmer J. and Kuklemeyer L. “Finite dynamic model for infinite media,” Journal of the Engineering Mechanics Division, 859-877, 1969

Marcellini A. et al. “The Benevento Seismic Risk Project. I – Seismotectonic and geotechnical background. Proc. V Int. Conf. on Seismic Zonation,” Nice, 1995

Matasovic N. “D-MOD_2. A computer program for seismic response analyses of horizontally layered soil deposits, earthfills dams and soil waste landfills,” GeoSyntec Consultants. Huntington Beach, California, 1995

Meletti C., Valensise G., Azzaro R., Barba S., Basili R., Galadini F., Gasperini P., Stucchi M. and Vannucci G. “Zonazione Sismogenetica ZS9. App.2 al Rapporto Conclusivo. – Gruppo di lavoro della mappa di pericolosità sismica (PCM n.3274/03), Istituto Nazionale di Geofisica e Vulcanologia (INGV), Rome, 2004 (in Italian)

Monteleone S. “Deformazioni gravitative profonde e grandi frane indotte dalle argille varicolori scagliose a Gerace e liquefazione nei terreni del territorio di Locri,” D.Sc. thesis, Università della Calabria, 1993 (in Italian)

Pagliaroli A. “Studio numerico e sperimentale dei fenomeni di amplificazione sismica locale di rilievi isolati,” Ph.D. thesis, Università La Sapienza di Roma, 2006 (in Italian)

Peruzza L., Pantosti D., Sleyko D. and Valensise G. (1997) – "Testing a New Hybrid Approach to Seismic Hazard Assessment: an Application to the Calabrian Arc (Southern Italy)," – Natural Hazards 14: 113-126, 1997

Petrucci O. and Polemio M. "Il dissesto della rupe di Gerace: patrimonio artistico e fattori idrogeologici di rischio," Convegno GEOBON, Torino, 2000 (in Italian)

Pugliese A. and Sabetta F. "Stima di spettri di risposta da registrazioni di forti terremoti italiani," Ingegneria Sismica, 6:2, 1989 (in Italian)

Rampello S., Silvestri F. and Viggiani G. "The dependence of small strain stiffness on stress state and history for fine-grained soils: the example of Vallericca clay," Proc. I Symp. on Pre-failure Deformations of Geomaterials, 1:273-279. Rotterdam: Balkema, 1994

Romeo R. and Delfino L. "CEDIT: Catalogo Nazionale degli effetti deformativi del suolo indotti da forti terremoti," Technical report SSN/RT/97/04, Department of Civil Protection, Rome, 1997 (in Italian)

Sabetta F. and Pugliese A. "Attenuation of peak horizontal acceleration and velocity from Italian strong motion records," Bulletin of the Seismological Society of America, 77(5), 1491–1513, 1987.

Seed H.B. and Idriss I.M. " Soil moduli and damping factors for dynamic response analysis", Report No. EERC70-10, Earthquake Engineering Research Center, Univ. of California, Berkeley, California, 1970

Wells, D.L., and Coppersmith K. J. "New Empirical Relationships among Magnitude, Rupture Lenght, Rupture Width, Rupture Area, and Surface Displacement," Bulletin of the Seismological Society of America, 84:974-1002, 1994